Sedimentation Kinetics of Flocculated Suspensions II: Sedimentation below the Critical Height

J. THURÖ CARSTENSEN* and KENNETH S. E. SU

Abstract □ Aside from the phenomenological equation by Egolf and McCabe and by Robinson, no attempts have appeared in literature in the past to quantitate terminal sedimentation characteristics of flocculated suspensions. The physical factors involved are suggested here, taking into account electrical effects and geometric factors contributing to friction. The equation of settling emerges as a linear combination of exponential decays—*viz.*, $[x - H_u] = A_1e^{-\omega_1\tau} + A_2e^{-\omega_2\tau}$, where x is the height of the sediment at time τ, H_u is the final height, and A and ω are constants. From the data it would appear that the friction, B, exerted is both viscosity (η) and dimension (R) dependent and of the form $B(\eta,R) = \Gamma \cdot e^{\xi\eta}e^{\mu R}$, where μ, ξ, and Γ are system-dependent constants.

Keyphrases □ Sedimentation kinetics—flocculated suspensions, equations □ Kinetics, sedimentation, flocculated suspensions—critical height, equations derived □ Suspensions, flocculated—sedimentation kinetics, equations

Sedimentation of flocculated suspensions has been the subject of several publications in the past (1–12); such systems have been shown (1, 7, 9–13) to sediment first at a rapid rate, primarily governed by gravitational and frictional forces. At a particular, well-reproducible point, the rate changes abruptly, and further sedimentation appears to be governed by forces over and above those just mentioned. With a few exceptions (1, 3, 13), all of the cited references attempt to modify Stokes's law to explain experimental data. In no case [except indirectly by Robinson (7)] has cognizance been taken of interparticle forces in relation to sedimentation rates.[1]

The treatment to follow deals with the second phase of sedimentation of flocculated suspensions of intermediate concentration, and attempts to account for the effect of such forces.

As shall be shown the final sedimentation pattern follows a linear combination of exponential decays. No previous treatment has led to such a pattern for the second stage of sedimentation or to the type plot encountered in concentrated suspensions, although the data in several examples in literature (2, 6, 7, 9) imply such a relationship.

THEORETICAL

London-van der Waals forces (14, 15) are responsible for the stability of the flocculated state, and in general, at small separations, the potential energy between two particles will be negative. At intermediate distances (16–19), however, the potential energy becomes positive because of the repulsion of double layers. Since the true charge of the particle surface cannot be determined by experiment, quantitation of such forces is difficult, and the upper limit for distances over which these forces will be effective cannot be stated *a priori*.

[1] A sizable amount of information regarding interparticle forces has been obtained by rheological approaches, notably the studies by Higuchi and Stehle (25), Gillespie (26, 27), Goodeve (28), and Vand (19).

Since the authors are dealing with the phase of sedimentation which occurs at a critical height, H_0, it may be advantageous, at the onset, to use a coordinate system slightly different from the one customarily used. Usually the position of the boundary is measured from the bottom of the tube and denoted x; time, t, is measured from the time sedimentation starts. Here, if the height H_0 occurs at time t_0, the position and time axes are chosen with the points t_0 and H_0 as the origin. Distance is now denoted y ($y = H_0 - x$), *i.e.*, positive in downward direction and positive for the times τ ($\tau = t - t_0$) in question. It shall be assumed that the center of gravity of the sediment is at one-half the height of the boundary of the sediment, *i.e.*, its position is $y = H_0/2$ originally, and at time τ it is $H_0 - x + x/2 = H_0 - x/2 = y$.

The forces exerted on the sediment are gravitational forces, frictional and reactional forces, and forces that are electrical in nature. The gravitational force is in the y-direction and of magnitude $M[1 - (\rho_0/\rho)]g$, where ρ and ρ_0 are the densities of solid and liquid, M is the mass of the sediment, and g is the gravitational acceleration. The frictional and reactional forces are in a direction opposite to y and must be related to viscosity and to wall and bottom effects, *i.e.*, to the geometry of the vessel. The functional relationship is not equated to $6\pi\eta r$, nor is an attempt made at this particular point in the development to formulate the diameter dependency, but the force is described as a velocity-dependent $[-B(\eta,R)dy/d\tau]$ and a velocity-independent $[-\psi(R)]$ component. The electrical force is assumed to be a repulsion (*i.e.*, in a direction opposite to the direction of the y-axis) and with regard to magnitude it is assumed to increase the closer the floc-aggregates are to one another; they are related to distance between flocs which in turn is related to the liquid volume of the cake, *i.e.*, $\pi R^2(x) - 4\pi r^3 n/3$, where R is the radius of the tube, and where n is the number and r the "radius" of the floc-aggregates. These forces are assumed to be of the form θy. The sum of all the forces then equals the mass of the sediment times its acceleration, *i.e.*,

$$M[1 - \rho_0/\rho]g - B(\eta,R)\frac{dy}{d\tau} - \psi(R) - \theta y = M\frac{d^2y}{d\tau^2} \quad \text{(Eq. 1)}$$

This may be rewritten

$$\frac{d^2y}{d\tau^2} + \frac{B(\eta,R)}{M}\frac{dy}{d\tau} + \frac{\theta}{M}y = [1 - \rho_0/\rho]g - \frac{\psi(R)}{M} \quad \text{(Eq. 2)}$$

It is apparent from inspection of Eqs. 1 and 2 that

$$y^* = \frac{M[1 - \rho_0/\rho]g - \psi(R)}{\theta}$$

is a particular solution to the differential equation. The remaining solutions are obtained by inserting an expected solution of the form $y = -A \cdot e^{-\omega\tau}$ into the homogeneous equation corresponding to Eq. 2. This yields:

$$-A \cdot e^{-\omega\tau}\left[\omega^2 - \frac{B(\eta,R)}{M}\omega + \frac{\theta}{M}\right] = 0 \quad \text{(Eq. 3)}$$

When the expression in brackets is equated to zero, Eq. 3 is satisfied; the characteristic roots are:

$$\omega = \frac{B(\eta,R)}{2M} \pm \sqrt{\left[\frac{B(\eta,R)}{2M}\right]^2 - \frac{\theta}{M}} \quad \text{(Eq. 4)}$$

The roots shown in Eq. 4 may be simplified if $B(\eta,R)/M \gg \theta/B(\eta,R)$ in which case they are:

$$\omega_1 = \frac{B(\eta,R)}{M} \quad \text{(Eq. 5)}$$

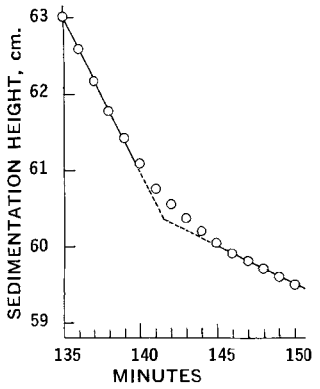

Figure 1—*Graph showing the method for determining the critical height* (H_0) *in a 5.54-cm. i.d. tube, 10% v/v glycerin and 11% w/v kaolin, and the critical time* (t_0).

and

$$\omega_2 = \frac{\theta}{B(\eta,R)} \qquad \text{(Eq. 6)}$$

The complete solution, in terms of y, is:

$$y = \frac{M[1 - \rho_0/\rho]g - \psi(R)}{\theta} - A_1' \cdot e^{-\omega_1 \tau} - A_2' \cdot e^{-\omega_2 \tau} \qquad \text{(Eq. 7)}$$

where the exponents in Eq. 7 have the meaning denoted in Eqs. 5 and 6. It is noted that $y^* = M[1 - \rho_0/\rho]g - \psi(R)/\theta$ corresponds to y_∞ by virtue of Eq. 7, and, therefore, is related to H_u, the ultimate height, by the relation $y_\infty = y^* = H_0 - H_u/2$. Inserting this into Eq. 7 and rearranging, yields:

$$x - H_u = A_1 e^{-\omega_1 \tau} + A_2 e^{-\omega_2 \tau} \qquad \text{(Eq. 8)}$$

where $A_1 = 2A_1'$ and $A_2 = 2A_2'$.

It is apparent from Eq. 8 that the terminal sedimentation pattern should be characterized by a linear combination of two exponential decays. By the assumption leading to Eqs. 5 and 6, $\omega_1 \gg \omega_2$ and the first term on the right hand side of Eq. 8 should be predominant at small values of τ and the last term should predominate at high values of τ.

EXPERIMENTAL

A previously described setup and methodology (1) were used: tubes 1.25 m. high, and of inside diameter 2.46, 2.72, 4.60, or 5.54 cm. were used as sedimentation vessels. The exact inside dimension was determined for each tube by introducing known amounts of water and checking heights with a precision cathetometer. The system studied was an 11% weight per volume kaolin[2] suspension

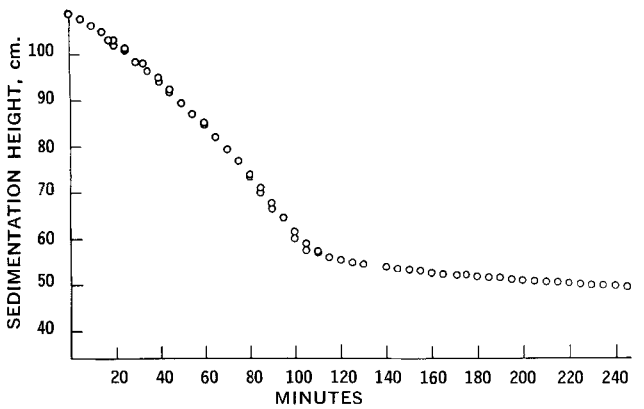

Figure 2—*Sedimentation curve of 11% w/v of kaolin in water in a tube of 5.54-cm. i.d. Duplicate points are shown.*

[2] Colloidal kaolin NF, lot No. 781603, Merck and Co., Rahway, N. J.

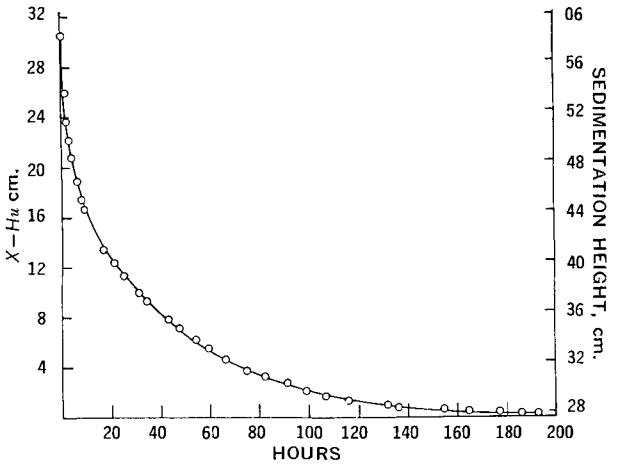

Figure 3—*Sedimentation pattern in a tube of 4.60-cm. i.d. of an 11% w/v suspension of kaolin in 5% v/v glycerin solution at heights below the critical height,* H_0. *The left ordinate is adjusted for final height,* H_u; *the right ordinate axis shows the actual heights* (x). *The curve shown in full is the theoretical curve;* $10 \cdot e^{-0.31\tau} + 20 \cdot e^{-0.0233\tau}$. *The points shown are experimental points.*

in water, 5% v/v glycerin, or 10% v/v glycerin. The suspensions were made in a Waring blender and transferred to the sedimentation tubes. The tops of the tubes were connected by means of a 24/40 ground joint to a stopcock, and after transfer, the stopcock was attached to the tube, and the suspension thoroughly deaerated by means of aspirator vacuum. Once deaerated, the tubes were turned end-over-end 10 times, the stopcock opened, the tube placed vertically and securely on a stand, and the position of the sedimentation boundary noted every 5 min.; timing intervals were made shorter when the critical height, H_0, was approached. This height, as well as the critical time, t_0, was then determined by graphical interpolation as shown in Fig. 1. Following this the position of the boundary was noted every 5 min. for 0.5 hr., and then hourly for 50 hr. (except for necessary schedule interruptions). Subsequently, the sedimentation height was recorded twice daily until a point in time had been reached where less than 0.2 mm. change occurred in a 24-hr. period; this usually required 7–13 days. Each set was obtained in duplicate. All sedimentation heights were determined by means of a cathetometer, and readings were accurate to 0.1 mm. The tubes used were not jacketed, but the experiments were carried out in a constant-temperature room at 25 ± 0.6°. The viscosity of the super-

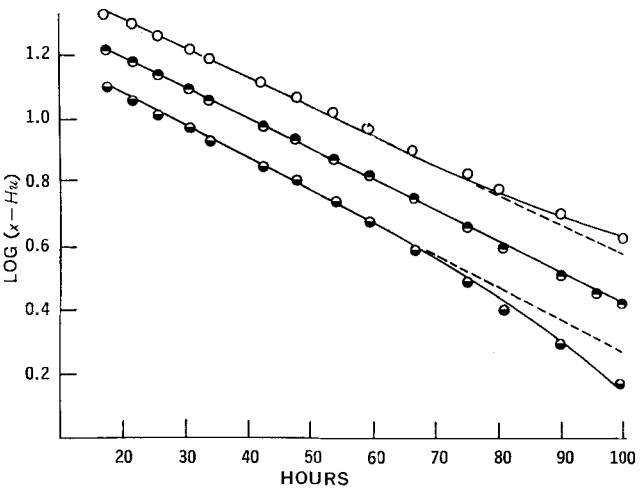

Figure 4—*Decay pattern of 11% w/v kaolin suspension in 5% v/v glycerin solution at high time values where* ω_2 *and* A_2 *predominate. Test was performed in a tube of 4.60-cm. i.d. The curves are separated by 0.1 and 0.2 logarithmic units as indicated. The plots demonstrate estimation of final sedimentation height prior to the time when it is reached. Key:* ○, H_u = *27.3 cm. (scale minus 0.2);* ◓, H_u = *27.8 cm. (scale minus 0.1), and* ◒, H_u = *28.4 cm.*

Table I—Theoretical Sedimentation Curve for 11% w/v Kaolin in 5% v/v Aqueous Glycerin in 4.6-cm. i.d. Tube[a]

Hr.	-0.137τ	$e^{-0.31\tau}$	$10e^{-0.31\tau}$	-0.097τ	$e^{-0.0223\tau}$	$20e^{-0.0223\tau}$	$10e^{-0.31\tau} + 20e^{-0.0223\tau}$
1	0.8630–1	0.730	7.30	0.9903–1	0.9780	19.56	26.86
2	0.7260–1	0.532	5.32	0.9806–1	0.9563	19.13	24.45
3	0.5890–1	0.388	3.88	0.9709–1	0.9352	18.70	22.58
4	0.4520–1	0.283	2.83	0.9612–1	0.9146	18.29	21.12
5	0.3150–1	0.207	2.07	0.9515–1	0.8944	17.89	19.96
6	0.1780–1	0.151	1.51	0.9418–1	0.8746	17.49	19.00
8	0.9280–2	0.085	0.85	0.9224–1	0.8361	16.72	17.57
10	0.6300–2	0.043	0.42	0.9030–1	0.8000	16.00	16.43
12	0.3560–2	0.023	0.23	0.8836–1	0.7649	15.30	15.53
14	0.2600–2	0.018	0.18	0.8642–1	0.7315	14.63	14.81
15	0.9450–3	0.009	0.09	0.8545–1	0.7164	14.33	14.42
20	0.260 –3	0.002	0.02	0.8060–1	0.6398	12.80	12.82
40				0.6120–1	0.4093	8.19	8.19
80				0.224 –1	0.1675	3.35	3.35
160				0.448 –2	0.0281	0.56	0.56

[a] $A_1 = 10$ cm., $\omega_1 = 0.31$ hr.$^{-1}$, $A_2 = 20$ cm., $\omega_2 = 0.0223$ hr.$^{-1}$.

natant was checked after each experiment by means of an Ostwald-Fenske viscometer.

RESULTS

A typical sedimentation curve is shown in Fig. 2; the shape is of the same nature as the one described elsewhere (1); the scale is selected so as to show both the initial and the beginning of the second phases of sedimentation, and the characteristic point separating the two curves. Even with the scale used it is apparent that some slight curvature exists in the second phase. In proper scale, all of the sedimentation curves have the shape shown in Fig. 3 when x is plotted as a function of τ.

Once the ultimate height, H_u, is attained, a first estimate of the parameters ω_2 and A_2 can be made, by using values of τ higher than 15 hr. In this case (as seen in Table I) $A_2e^{-\omega_2\tau} \gg A_1e^{-\omega_1\tau}$ and Eq. 8 becomes $[x - H_u] = A_2e^{-\omega_2\tau}$. The logarithmic form of this is

$$\log [x - H_u] = -\frac{\omega_2}{2.3}\tau + \log A_2 \ (\tau > 15 \text{ hr.}) \quad \text{(Eq. 9)}$$

An example of this is shown in Table II and Fig. 4. It should be noted that the final height may be estimated well in advance of its actual occurrence from linearity as opposed to curvature of this type plot. Estimated values were always within 0.5 mm. of the actual, experimentally determined, final height.

By means of the estimates of A_2 and ω_2 the value of $[x - H_u] - A_2e^{-\omega_2\tau}$ can be determined at values of τ less than 15 hr., so the two other parameters may be estimated by rearrangement of Eq. 8:

$$\log \{[x - H_u] - A_2e^{-\omega_2\tau}\} = -\frac{\omega_1}{2.3}\tau + \log A_1 \quad \text{(Eq. 10)}$$

An example of this is shown in Table III and Fig. 5. By this plotting a better estimate of A_2 is obtained as shown in Fig. 5. The difference between this estimate and the original estimate was always within error of the graphical estimate in Fig. 4. With the estimates of A_1, ω_1, A_2, and ω_2, statistically best values may be obtained by computer, using iteration techniques (20–22). It should be noted, however, that graphical and manually generated estimates are quite good. Construction of the theoretical curve from the parameter estimates arrived at in Tables II and III and Figs. 4 and 5 is shown in Table I, and the curve drawn in full in Fig. 3 is taken from this table. It is quite obvious from the figure that the data fit the curve well. Averages of duplicate determinations of A_1, ω_1, A_2, and ω_2 from all the sedimentation tests are listed in Table IV.

DISCUSSION

In not too concentrated suspensions the sedimentation pattern is characterized first by a settling pattern which is linear (9) or parabolic with time (1) caused, respectively, by free fall or constant-density plug descent (1, 9). Attempts to describe mathematically the phase that follows the initial settling have been made by Robinson (7) and by Egolf and McCabe (13). Robinson found the dependency of the initial settling rates on concentration and then

Table II—Sedimentation Data for High Values of τ when ω_2 and A_2 Are the Predominant Terms

Hr.	Height, x, cm.	$x - 28.4$, cm.	log $[x - 28.4]$	$x - 27.8$, cm.	log $[x - 27.8]$	$x - 27.3$, cm.	log $[x - 27.3]$
17.67	41.06	12.76	1.1059	13.36	1.1258	13.86	1.1318
21.50	40.02	11.62	1.0652	12.22	1.0871	12.72	1.1045
25.65	38.96	10.56	1.0237	11.16	1.0477	11.66	1.0630
30.42	37.88	9.48	0.9768	10.08	1.0035	10.58	1.0245
34.20	37.12	8.72	0.9405	9.32	0.9694	9.82	0.9921
42.70	35.56	7.16	0.8549	7.76	0.8899	8.26	0.9170
47.22	34.87	6.47	0.8109	7.07	0.8494	7.57	0.8791
53.98	33.90	5.50	0.7404	6.10	0.7853	6.60	0.8195
59.30	33.23	4.83	0.6840	5.43	0.7348	5.93	0.7731
66.70	32.32	3.92	0.5933	4.52	0.6551	5.02	0.7007
75.23	31.51	3.11	0.4928	3.71	0.5694	4.21	0.6243
82.30	30.93	2.53	0.4031	3.13	0.4955	3.63	0.5599
90.18	30.39	1.99	0.2989	2.59	0.4133	3.09	0.4900
98.90	39.90	1.50	0.1761	2.10	0.3222	2.60	0.4150
107.12				1.70			
115.55				1.34			
132.23				0.92			
136.70				0.70			
155.12				0.52			
165.17				0.41			
176.93				0.32			
186.00				0.20			
193.50				0.19			

Table III—Sedimentation Data at Low Values of τ[a]

Hr.	Height, x, cm.	$[x - 27.8]$, cm.	0.0097τ	$Q = e^{-0.0223\tau}$	$[x-27.8-19.2Q]$, cm.	$[x-27.8-20Q]$, cm.	$[x-27.8-20.5Q]$, cm.
0	58.3	30.5	0	1	11.3	10.5	10.0
0.27	56.55	28.75	0.9974–1	0.9940	9.67	8.87	8.37
0.52	55.33	27.53	0.9950–1	0.9885	8.55	7.76	7.27
1.30	52.87	25.07	0.9874–1	0.9714	6.42	5.64	5.16
1.97	51.41	23.61	0.9809–1	0.9570	5.24	4.47	3.99
2.47	50.56	22.76	0.9760–1	0.9463	4.59	3.83	3.36
2.92	49.85	22.05	0.9717–1	0.9369	4.06	3.31	2.84
3.48	49.15	21.35	0.9662–1	0.9252	3.59	2.85	2.38
4.05	48.49	20.69	0.9607–1	0.9135	3.15	2.42	1.96
4.52	48.01	20.21	0.9562–1	0.9040	2.85	2.13	1.68
5.02	47.54	19.74	0.9513–1	0.8939	2.58	1.86	1.42
5.52	47.12	19.32	0.9465–1	0.8840	2.35	1.64	1.20
6.03	46.68	18.88	0.9415–1	0.8740	2.10	1.40	0.96
6.50	46.33	18.53	0.9370–1	0.8648	1.93	1.23	0.80
7.02	45.96	18.16	0.9319–1	0.8549	1.75	1.06	0.63
7.45	45.66	17.88	0.9277–1	0.8466	1.63	0.95	0.52
8.03	45.32	17.52	0.9221–1	0.8358	1.47	0.80	0.39
8.62	44.97	17.17	0.9164–1	0.8249	1.33	0.67	0.20
9.45	44.50	16.70	0.9083–1	0.9097	1.15	0.51	0.10

[a] Eleven percent w/v of kaolin in 5% v/v glycerin in a tube of 4.60-cm. i.d.

applied these findings to experimental data; since in that context, the sedimentation volume represents a suspension of time-dependent concentration (disregarding the supernatant) the settling rates should constantly change in a predictable fashion.

Egolf and McCabe suggested a phenomenological log–log relationship between absolute height and time for the phase following the initial settling. Ward and Kammermeyer (8) tested both models in different type systems (carbonates, silica, and magnesium oxide), and found fair agreement with regard to the shape of the curves, but large (20–40%) quantitative deviations in the second phase of sedimentation. These authors concluded that the application of the approaches of Robinson (7) and Egolf and McCabe (13) is limited to prediction of settling of only such systems that are closely related to the ones used to develop the appropriate equations and factors. Reflecting on the later findings that the initial settling is in the form of a constant-density plug (1, 9–11), it would appear that it may be erroneous to assume that the sediment may be viewed as a uniform suspension of constantly changing concentration; this may be the source of the cited quantitative deviations.

The approach taken here is to account for the forces involved (even though all of them cannot be expressed explicitly *a priori*) and then to try to gain insight into them, quantitatively and qualitatively, by way of experimental results. Experimental variation limits the number of conclusions that may be drawn from the A_1- and ω_1-values. It will be noted from Table IV that the coefficient of variation for these two parameters is 5%; this prohibits any conclusions that may be drawn regarding the viscosity dependency of ω_1 (and, therefore, also of $B[\eta,R]$). The data would imply that either ω_1 does not vary with changing R, or, possibly, it decreases with increasing R.

On the other hand, ω_2 is quite reproducible (±1%); it appears from the results in Table IV that $\omega_2\{\omega_2 = \theta \cdot [B(\eta,R)]^{-1}\}$ decreases with both increasing R- and η-values, and suggest the radial dependence of $B(\eta,R)$ to be of the form $e^{\mu R}$; in this case Eq. 6 takes the form:

$$\log \omega_2 = \log \theta - \log C^* - \frac{\mu}{2.3} R \qquad \text{(Eq. 11)}$$

where C^* is a constant. Figure 6 shows the data plotted in this fashion, and the plots are fairly linear; the slopes (calculated by least-squares fit of the data in Table IV) are shown in Table V, and are, as seen, fairly close to one another.

The data in Table IV would also suggest the dependence of ω_2 on viscosity to be an exponential decay; if this is the case, then $B(\eta,R) = \Gamma \cdot e^{\mu R} e^{\zeta \eta}$; inserting this in Eq. 6 yields:

$$\log \omega_2 = \log \frac{\theta}{\Gamma} - \frac{\mu}{2.3} R - \frac{\zeta}{2.3}\eta \qquad \text{(Eq. 12)}$$

If $\log \omega_2$ is plotted as a function of viscosity, four straight lines should result, one for each tube. The data plotted in this fashion are shown in Fig. 7. It is seen that fairly good linearity is exhibited, and the values of the slopes as shown in Table V are close to each other. Least-squares values of the intercepts from Figs. 6 and 7 are also shown in this table. The intercepts in Fig. 6 should be $[2 + \log \theta/\Gamma - (\mu \cdot R/2.3)]$ and the intercepts in Fig. 7 should be $[2 + \log \theta/\Gamma - (\zeta \cdot \eta/2.3)]$. It is, therefore, possible to get a crude estimate of $\log [\theta/\Gamma]$ by means of the intercept values. Results of this type calculation are shown in Table V and values derived from the

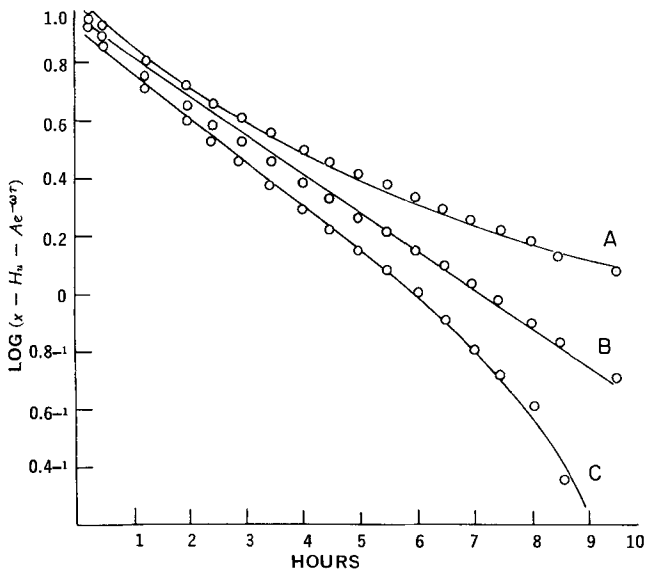

Figure 5—*Decay pattern of 11% w/v kaolin suspension in 5% v/v glycerin solution at low time values where ω_1 and A_1 predominate. Data pertain to 4.60-cm. i.d. tube. The plots demonstrate refinement of the estimate of A_2. Key: A, A_2 = 19.2 cm.; B, A_2 = 20.0 cm.; and C, A_2 = 20.5 cm.*

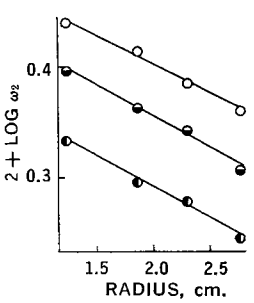

Figure 6—*Plot of the logarithm of the smaller characteristic root, ω_2, as a function of the tube diameter. ○, 0.89 cps.; ◒, 1.05 cps.; ◐, 1.20 cps.*

Table IV—Value of A_1, A_2, ω_1, and ω_2 as a Function of Viscosity and Tube Diameter

Glycerin, % v/v	Viscosity, poises	Radius, cm.	A_1, cm. ±10%	ω_1, hr.$^{-1}$ ±10%	A_2, cm. ±6%	ω_2, hr.$^{-1}$ ±1%
0	0.0089	1.23	4.9	0.42	24.1	0.0276
0	—	1.86	10.3	0.38	16.0	0.0260
0	—	2.30	10.2	0.29	18.7	0.0242
0	—	2.77	8.2	0.13	20.0	0.0229
5	0.0105	1.23	6.0	0.41	31.2	0.0248
5	—	1.86	9.3	0.38	31.3	0.0230
5	—	2.30	10.0	0.31	20.5	0.0220
5	—	2.77	9.8	0.29	18.6	0.0202
10	0.0120	1.23	7.1	0.38	41.0	0.0216
10	—	1.86	9.6	0.30	19.3	0.0197
10	—	2.30	8.6	0.33	17.4	0.0190
10	—	2.77	8.8	0.15	20.0	0.0175

Table V—Slopes and Intercepts from Figs. 6 and 7

Line	Fig.	Slope (ζ/2.3), cps.$^{-1}$	Slope (μ/2.3), cm.$^{-1}$	Intercept	log [θ/Γ]
R = 1.23 cm.	7	−0.36		0.77	0.84–2[a]
R = 1.86 cm.	7	−0.40		0.78	0.88–2[a]
R = 2.30 cm.	7	−0.35		0.70	0.82–2[a]
T = 2.77 cm.	7	−0.39		0.71	0.86–2[a]
η = 0.89 cps.	6		−0.054	0.51	0.88–2[b]
η = 1.05 cps.	6		−0.057	0.46	0.85–2[b]
η = 1.20 cps.	6		−0.057	0.40	0.84–2[b]

[a] Based on an average value of μ/2.3 = 0.055. [b] Based on an average value of ζ/2.3 = 0.37.

two figures show acceptably good agreement, especially considering that they have been obtained from extrapolated figures (intercepts).

This fact in combination with the linearity of the plots in Figs. 6 and 7, the closeness of the values of the slopes, and the adherence of all the data to an equation of the type of Eq. 8 lends credence to the views presented here.

It should be mentioned, qualitatively, that increasing concentrations tend to decrease (or mask) the values of A_1, and that this parameter eventually is of such small magnitude that it can no longer be detected within experimental error. In the same vein, H_0 becomes larger with increasing solids content and, eventually, at a critical concentration the initial constant-density plug phase will disappear, and at a second critical concentration, the A_1-term will disappear. The entire sedimentation pattern will then be a simple logarithmic decay curve. The critical concentration for kaolin in 10% v/v glycerin in a tube of 2.5-cm. i.d. is 8–10 w/v percent. Data of this nature have been reported occasionally in literature in the past, the data by Haines and Martin (6) being a notable example.

The final height, H_u, as reported here, may still be subject to some decrease by consolidation processes such as described by Ratcliff (23, 24). This phase has not been a subject of this investigation.

SUMMARY

The sedimentation of flocculated suspensions takes place in successive stages; the sedimentation phase following the initial phase has been studied and found, based on consideration of the forces involved, to be confined to follow the following equation: $[x-H_u] = A_1e^{-\omega_1\tau} + A_2e^{-\omega_2\tau}$. Experimental data have supported the presented concepts and suggest that the frictional term in the equation of motion is of the form $B(\eta,R) = \Gamma \cdot e^{\mu R}e^{\zeta\eta}$.

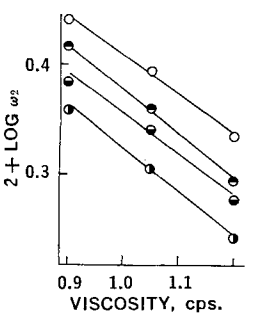

Figure 7—*Plot of the logarithm of the smaller characteristic root, ω_2, as a function of viscosity. Key: ○, 2.46-cm. i.d. tube; ◓, 3.72-cm. i.d. tube; ◒, 4.60-cm i.d. tube; and ◑, 5.54-cm. i.d. tube.*

NOMENCLATURE

A, A_1, A_2, A_1', A_2'	= preexponential factors in descent of sedimentation boundary
$B(\eta,R)$	= viscosity dependent component of frictional force
C^*	= preexponential factor for radial dependence of ω_2
g	= gravitational acceleration
H_0	= critical height
M	= mass of sediment
r	= radius of floc
R	= radius of tube
t	= time measured from start of sedimentation
t_0	= critical time
x	= height of sedimentation boundary above bottom of tube
y	= distance of sedimentation boundary from critical height ($= H_0 - x/2$)
y_∞, y^*	= y-value at infinite time ($= H_0 - H_u/2$)
$\psi(R)$	= viscosity independent component of frictional force
ρ_0	= density of fluid
ρ	= density of suspended solid
τ	= time measured from critical time ($= t - t_0$)
μ	= exponential factor to radial dependence of ω_2
Γ	= preexponential factor to radial dependence of ω_2
θ	= dimensional factor in electrical repulsion term
ζ	= exponential factor to viscosity dependence of ω_2
ω, ω_1, ω_2	= exponential decay constants in descent of sedimentation boundary

REFERENCES

(1) J. T. Carstensen and K. Su, *J. Pharm. Sci.*, **59**, 666(1970).
(2) R. Stokes, *Proc. Cambridge Phil. Soc.*, **9**, 5(1856).
(3) G. Kynch, *Trans. Faraday Soc.*, **48**, 166(1952).
(4) H. Steinour, *Ind. Eng. Chem.*, **36**, 840(1944).
(5) *Ibid.*, **35**, 901(1944).
(6) B. A. Haines, Jr., and A. N. Martin, *J. Pharm. Sci.*, **50**, 228 (1961).
(7) C. S. Robinson, *Ind. Eng. Chem.*, **18**, 869(1926).

(9) A. S. Michaels and J. C. Bolger, *Ind. Eng. Chem. Fundam.*, **1,** 24(1962).
(10) A. M. Gaudin and M. C. Fuerstenau, *Eng. Mining J.*, **159,** 110(1958).
(11) A. M. Gaudin and M. C. Fuerstenau, *Int. Mining Proc. Congr.*, London, England, Apr. 1960.
(12) A. M. Gaudin, M. C. Fuerstenau, and S. R. Mitchell, *Mining Eng. (London)*, **11,** 613(1959).
(13) C. B. Egolf and W. L. McCabe, *Trans. Amer. Inst. Chem. Eng.*, **33,** 620(1937).
(14) J. deBoer, *Advan. Colloid Interface Sci.*, **3,** 21(1950).
(15) F. London, *Z. Phys.*, **63,** 245(1930).
(16) B. Deryagin, A. Titijevskaia, I. Abriscova, and E. Lifshitz, *Discuss. Faraday Soc.*, **18,** 24(1954).
(17) B. Deryagin, I. Abriscova, and E. Lifshitz, *Quart. Rev. (London)*, **10,** 295(1956).
(18) E. Verway and J. Overbeek, "Theory of the Stability of Lyophobic Colloids," Elsevier, Amsterdam, The Netherlands, 1948.
(19) V. Vand, *J. Phys. Colloid Chem.*, **52,** 277(1948).
(20) C. R. Wylie, Jr., "Advanced Engineering Mathematics," McGraw-Hill, New York, N. Y., 1960, p. 177.
(21) C. M. Metzler, APhA Academy of Pharmaceutical Sciences, 5th National Meeting, Washington, D. C., November 20, 1968.
(22) J. T. Carstensen, J. B. Johnson, D. C. Spera, and M. J. Frank, *J. Pharm. Sci.*, **57,** 23(1968).
(23) G. A. Ratcliff, D. A. Blackader, and D. N. Sutherland, *Chem. Eng. Sci.*, **22,** 201(1967).
(24) G. A. Ratcliff, *J. Colloid Interface Sci.*, **25,** 586(1967).
(25) W. Higuchi and R. G. Stehle, *J. Pharm. Sci.*, **54,** 265(1965).
(26) T. Gillespie, *J. Phys. Chem.*, **66,** 1077(1962).
(27) T. Gillespie, *J. Colloid Sci.*, **15,** 219(1960).
(28) C. F. Goodeve, *Trans. Faraday Soc.*, **35,** 342(1939).

ACKNOWLEDGMENTS AND ADDRESSES

Received August 21, 1969, from the *School of Pharmacy and Extension Services in Pharmacy, University Extension, University of Wisconsin, Madison, WI 53706*

Accepted for publication November 14, 1969.

This investigation was supported by grants from R. T. Vanderbilt Co., New York, NY 10017 and Hoffmann-La Roche, Inc., Nutley, NJ 07110

* To whom requests for reprints should be addressed.

Cholesterol Biosynthesis and Lipid Biochemistry in the Scolex of *Echinococcus granulosus*

GEORGE A. DIGENIS*, RALPH E. THORSON†, and ARPINE KONYALIAN

Abstract □ When live scolices of *Echinococcus granulosus* were incubated with labeled mevalonate *in vitro*, no radioactivity was incorporated into the parasites' cholesterol fraction. However, labeled cholesterol was recovered after a scolices' homogenate was incubated with 4-^{14}C-cholesteryl acetate. It is suggested that the scolex of *E. granulosus* is unable to biosynthesize cholesterol and that it obtains cholesterol in an esterified form from the host, which is subsequently hydrolyzed within the scolex to free cholesterol. The fatty acid content of *E. granulosus* was examined by gas-liquid chromatography.

Keyphrases □ *Echinococcus granulosus* scolices—cholesterol biosynthesis □ Cholesterol biosynthesis—*E. granulosus* scolices □ Lipid biochemistry—*E. granulosus* scolices □ Hydrolytic activity, *E. granulosus* scolices—4-^{14}C-cholesteryl acetate □ TLC—separation □ GLC—identity □ Scintillometry—analysis

It is a well-known fact that, in vertebrates, cholesterol is biosynthesized from acetate or mevalonate. In many insects, however, radioactive acetate or mevalonate is not incorporated into cholesterol; some insects do not even synthesize squalene, the noncyclic precursor of sterols (1, 2).

In 1954, Butenandt and Karlson (3) first isolated 25 mg. of ecdysone, the molting hormone, from 500 kg. of silkworm pupae. The compound [shown later to be a steroid (4)] was effective in accelerating molting, even in quantities below 7.5×10^{-3} mcg., when injected into ligated fly abdomens. In 1963, Karlson and Hoffmeister (5) demonstrated the incorporation of radioactivity from tritium-labeled cholesterol into ecdysone in *Calliphora* larvae, indicating that cholesterol is a precursor to ecdysone. Clark and Bloch (6) showed that 95% of the dietary cholesterol in the beetle *Dermestes vulpinus* could be replaced by β-sitosterol for structural utilization, but 5% of it remained essential for metabolic function; Clayton (7), working with the cockroach *Blattella germanica*, obtained similar results. According to Karlson (8), only a small part of the cholesterol injected into insects was converted to ecdysone; the majority still fulfilled cellular functions. Smissman *et al.* (9) isolated dehydroepiandrosterone, pregnenolone, and progesterone as the products of normal insect metabolism of dietary sterols in the confused flour beetle, *Tribolium confusum*. Horn *et al.* (4) isolated crustecdysone from crayfish, a compound which proved to be both chemically and biologically similar to ecdysone. Carlisle (10) demonstrated the biological activity of extracts from crabs, copepods, and locusts on the immature shore crab *Carcinus maenas*, indicating the presence of a common set of interactive ecdysones in crustaceans and insects.

The hormone that has an effect opposite to that of ecdysone on the molting stages of insects was first isolated from the abdomens of *Cecropia* males by Williams (11). Karlson and Schmialek (12) injected extracts of the excretions of the beetle *Tenebrio molitor* into mature larvae of the same species and noted the retardation of pupation in 88% of the treated larvae. In